Materials Chemistry and Physics 125 (2011) 628–640

Contents lists available at ScienceDirect

Materials Chemistry and Physics

journal homepage: www.elsevier.com/locate/matchemphys

Corrosion inhibition of 6061 Al–15 vol. pct. SiC(p) composite and its base alloy in a mixture of sulphuric acid and hydrochloric acid by 4-(N,N-dimethyl amino) benzaldehyde thiosemicarbazone

Geetha Mable Pinto[a], Jagannath Nayak[b], A. Nityananda Shetty[a,*]

[a] Department of Chemistry, National Institute of Technology Karnataka, Surathkal, Srinivasnagar 575 025, Mangalore, Karnataka, India
[b] Department of Metallurgical and Materials Engineering, National Institute of Technology Karnataka, Surathkal, Srinivasnagar 575 025, Karnataka, India

ARTICLE INFO

Article history:
Received 10 December 2009
Received in revised form 2 September 2010
Accepted 7 October 2010

Keywords:
A. Alloys
C. Electrochemical techniques
D. Adsorption
D. Corrosion

ABSTRACT

The corrosion inhibition characteristics of 4-(N,N-dimethylamino) benzaldehyde thiosemicarbazone (DMABT) on the corrosion behavior of 6061 Al–15 vol. pct. SiC(p) composite and its base alloy were studied at different temperatures in acid mixture medium containing varying concentrations of hydrochloric acid and sulphuric acid using Tafel extrapolation technique and ac impedance spectroscopy (EIS). The effect of inhibitor concentration, temperature and concentration of the acid mixture media on the inhibitor action was investigated. It was found that inhibition efficiencies increase with the increase in inhibitor concentration, but decrease with the increase in temperature and with the increase in concentration of the acid media. Thermodynamic parameters for dissolution process were determined. The adsorption of DMABT on both the composite and base alloy was found to be through physisorption obeying Freundlich adsorption isotherm.

1. Introduction

Reinforcing 6061 Al alloy with SiC particles results in their better performance [1,2]. Aluminum matrix composites (AMCs) have received considerable attention for military, automobile and aerospace applications because of their low density, high strength and high stiffness [3–9]. One of the main drawbacks in the use of metal matrix composite is the decrease in corrosion resistance compared to the base alloy. For the base alloy, protective oxide surface film imparts corrosion resistance; but, addition of a reinforcing phase could lead to discontinuities in the film, thereby increasing the number of sites where corrosion can be initiated and making the composites more vulnerable [8,10]. However, the high corrosion rates of these composites, particularly in acid media can be combated using inhibitors [11,12]. Due to the wide applications of such composites, they frequently come in contact with acid during cleaning, pickling, descaling, etc. The inhibition of aluminum corrosion in acid solutions was extensively studied using organic and inorganic compounds. It has been reported that the addition of chloride ions to sulphate solutions enhances aluminum corrosion [13]. A wide variety of compounds are used as inhibitors in acid media. These are mainly organic compounds containing N, S or O atoms [14–16] and critical use of these compounds in industries has also been reviewed [17–19]. Organic compounds containing both N and S atoms function as better adsorption inhibitors because of their lone pair of electrons and polar nature of the molecules [20,21].

The present work aims at investigating the inhibitive action of 4-(N,N-dimethyl amino) benzaldehyde thiosemicarbazone (DMABT) on the corrosion of 6061 Al–15 vol. pct. SiC(p) composite and its base alloy in acid media containing hydrochloric acid and sulphuric acid at different concentration levels of the acids as well as at different temperatures. The investigations were carried out using electrochemical techniques such as potentiodynamic polarization and electrochemical impedance spectroscopy (EIS) techniques. Corrosion parameters were derived in the presence and absence of the inhibitor and inhibition efficiency was calculated in different acid mixture concentrations.

2. Experimental

2.1. Material

The experiments were performed with specimens of 6061 Al–15 vol. pct. SiC(p) composite and its base alloy in extruded rod form (extrusion ratio 30:1). The composition of the base metal 6061 Al alloy is given in Table 1. Cylindrical test coupons were cut from the rods and sealed with epoxy resin in such a way that the areas of the composite and the base alloy exposed to the medium were 0.95 cm^2 and 0.785 cm^2, respectively. These coupons were polished as per standard metallographic practice, belt grinding followed by polishing on emery papers, and finally on polishing wheel using levigated alumina to obtain mirror finish. It was then degreased with acetone,

* Corresponding author. Tel.: +91 824 2474200/9448779922; fax: +91 824 2474033.
E-mail address: nityashreya@gmail.com (A.N. Shetty).

0254-0584/$ – see front matter © 2010 Elsevier B.V. All rights reserved.
doi:10.1016/j.matchemphys.2010.10.006

Table 1
The composition of the base metal Al 6061 alloy.

Element	Cu	Si	Mg	Cr	Al
Composition (wt.%)	0.25	0.6	1.0	0.25	97.9

washed with double distilled water and dried before immersing in the corrosion medium.

2.2. Medium

Standard solutions of hydrochloric acid and sulphuric acid mixture were prepared from analytical grade (Nice) acids by mixing them in 2:1 molar ratio. The three solutions used for the study were with the following concentrations of hydrochloric acid and sulphuric acid, respectively: 0.5 M + 0.25 M, 1 M + 0.5 M and 2 M + 1 M. Experiments were carried out using calibrated thermostat at temperatures 30 °C, 35 °C, 40 °C, 45 °C, 50 °C (±0.5 °C). The inhibitive effect was studied by introducing 50–1000 ppm (0.2–4 mM) of DMABT into the acid mixture solutions.

2.3. Electrochemical measurements

2.3.1. Tafel polarization studies

Electrochemical measurements were carried out using electrochemical work station, Auto Lab 30 and GPES software. Tafel plot measurements were carried out using conventional three electrode Pyrex glass cell with platinum counter electrode and saturated calomel electrode (SCE) as reference electrodes. All the values of potential are therefore referred to the SCE. Finely polished composite and base alloy specimens were exposed to corrosion medium of different concentrations of hydrochloric acid–sulphuric acid mixtures at different temperatures (30–50 °C) and allowed to establish a steady state open circuit potential. The potentiodynamic current–potential curves were recorded by polarizing the specimen to −250 mV cathodically and +250 mV anodically with respect to open circuit potential (OCP) at scan rate of 1 mV s^{-1}.

2.3.2. Electrochemical impedance spectroscopy (EIS) studies

The corrosion behaviors of the specimens of the composite and the base alloy were also obtained from EIS technique using electrochemical work station, Auto Lab 30 and FRA software. In EIS technique a small amplitude ac signal of 10 mV and frequency spectrum from 100 kHz to 0.01 Hz was impressed at the OCP and impedance data were analyzed using Nyquist plots. The charge transfer resistance, R_t, was extracted from the diameter of the semicircle in Nyquist plot.

In all the above-mentioned measurements, at least three similar results were considered and their average values are reported.

2.4. Synthesis of 4-(N,N-dimethyl amino) benzaldehyde thiosemicarbazone

4-(N,N-dimethylamino) benzaldehyde thiosemicarbazone was synthesized and recrystallised as per the reported procedure [22]. A mixture containing equimolar ethanolic 4-(N,N-dimethylamino) benzaldehyde and thiosemicarbazone was taken in a round-bottomed flask. The reaction mixture was refluxed on a hot water bath for about 60 min. The pale yellow colored product obtained was separated by filtration and dried. The product was recrystallised from ethanol. The purity of the recrystallised product was checked by IR, elemental analysis and melting point.

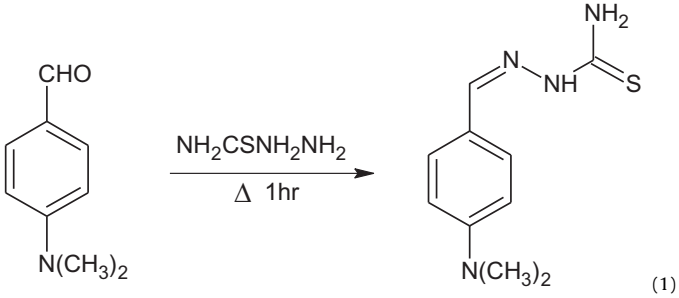

(1)

2.5. Scanning electron microscopy (SEM) analysis

The scanning electron microscopic images and EDX spectra of the samples were recorded using JEOL JSM – 6380 LA analytical scanning electron microscope.

3. Results and discussion

3.1. Potentiodynamic polarization (PDP) measurements

The polarization studies of aluminum specimens were carried out in three different solutions containing 0.5 M, 1 M, 2 M hydrochloric acid and 0.25 M, 0.5 M, 1 M sulphuric acid, respectively, in the absence and in the presence of different concentrations of DMABT (50–1000 ppm). Figs. 1 and 2 represent potentiodynamic polarization curves of 6061 Al–SiC composite and its base alloy for various concentrations of DMABT in a solution containing 2 M hydrochloric acid and 1 M sulphuric acid solutions at 30 °C in the absence and in the presence of DMABT. Similar results were obtained in the same concentrations of acid mixtures at four other temperatures and also in the other two concentrations of the acid mixtures at the five temperatures studied. The electrochemical parameters (E_{corr}, i_{corr}, b_a and b_c) associated with the polarization measurements at different DMABT concentrations as well as at different temperatures for the composite and the base alloy in three different concentrations of the acid mixture are listed in Tables 2–4. Since the plateau of anodic current is not well defined, the corrosion current density values in all the above cases were determined by the extrapolation of cathodic Tafel slopes to the respective corrosion potentials.

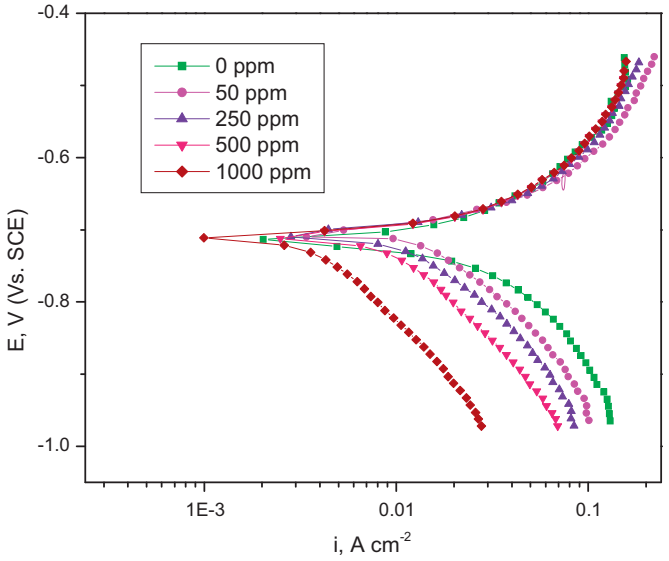

Fig. 1. Tafel polarization curves for the corrosion of composite in 2 M HCl + 1 M H_2SO_4 mixture at 30 °C in the presence of different concentrations of DMABT.

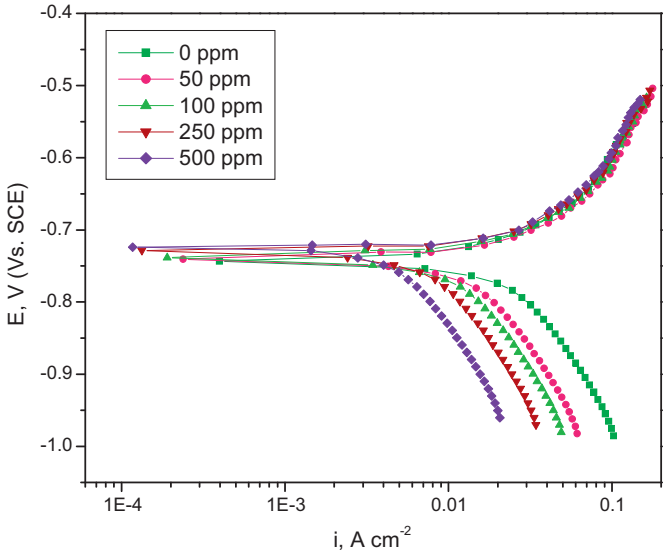

Fig. 2. Tafel polarization curves for the corrosion of base alloy in 2 M HCl + 1 M H_2SO_4 mixture at 30 °C in the presence of different concentrations of DMABT.

Table 2
Electrochemical parameters obtained from PDP measurements of Al composite and its base alloy in 2 M hydrochloric acid and 1 M sulphuric acid mixture in the absence and presence of various concentrations of DMABT.

Temp. of medium (°C)	Composite					Base alloy				
	Conc. of inhibitor in ppm	I_{cor} ($\times_{10}{}^{-3}$ A cm^{-2})	$-b_c$ (mV dec^{-1})	E_{corr} (mV SCE^{-1})	IE%	Conc. of inhibitor in ppm	I_{cor} ($\times_{10}{}^{-3}$ A cm^{-2})	$-b_c$ (mV dec^{-1})	E_{corr} (mV SCE^{-1})	IE%
30	0	12.63	86	−716		0	8.52	74	−743	
	50	7.12	110	−715	43.6	50	5.23	90	−741	38.6
	250	5.80	136	−714	54.1	100	4.41	97	−740	48.2
	500	3.51	140	−711	72.2	250	3.40	105	−738	60.1
	1000	1.26	148	−712	90.0	500	2.18	124	−736	74.4
35	0	16.72	80	−719		0	11.49	68	−747	
	50	10.02	98	−719	40.1	50	7.40	77	−746	35.6
	250	8.56	116	−715	48.8	100	6.41	91	−744	44.2
	500	6.03	128	−713	63.9	250	5.18	105	−742	54.9
	1000	2.21	137	−710	86.8	500	3.46	130	−741	69.9
40	0	21.95	74	−725		0	13.82	63	−750	
	50	13.97	92	−724	36.4	50	9.51	79	−749	31.2
	250	11.55	98	−720	47.4	100	8.54	86	−747	38.2
	500	9.42	112	−718	57.1	250	7.00	101	−745	49.3
	1000	5.52	126	−719	74.9	500	4.88	115	−740	64.6
45	0	31.02	65	−730		0	15.40	58	−752	
	50	23.11	85	−729	25.5	50	12.20	75	−749	24.8
	250	19.31	96	−728	37.7	100	10.43	86	−746	32.0
	500	16.40	106	−725	47.8	250	8.8	95	−747	42.6
	1000	10.98	112	−724	64.6	500	6.27	109	−744	59.1
50	0	38.05	60	−736		0	16.58	55	−759	
	50	29.78	76	−735	21.7	50	13.31	66	−758	19.7
	250	26.25	92	−734	31.0	100	12.11	77	−755	27.0
	500	22.03	98	−733	42.1	250	10.82	88	−750	34.7
	1000	16.52	105	−730	56.6	500	7.90	100	−750	52.4

Table 3
Electrochemical parameters obtained from PDP measurements of Al composite and its base alloy in 1 M hydrochloric acid and 0.5 M sulphuric acid mixture in the absence and presence of various concentrations of DMABT.

Temp. of medium (°C)	Composite					Base alloy				
	Conc. of inhibitor (ppm)	I_{cor} ($\times_{10}{}^{-3}$ A cm^{-2})	$-b_c$ (mV dec^{-1})	E_{corr} (mV SCE^{-1})	IE%	Conc. of inhibitor (ppm)	I_{cor} ($\times_{10}{}^{-3}$ A cm^{-2})	$-b_c$ (mV dec^{-1})	E_{corr} (mV SCE^{-1})	IE%
30	0	9.01	109	−679		0	3.22	109	−714	
	50	5.45	120	−676	39.5	50	2.06	127	−714	36.0
	250	4.04	128	−676	55.2	100	1.72	135	−713	46.6
	400	2.80	141	−675	68.9	200	1.00	146	−712	68.9
	600	2.02	153	−674	77.6	250	0.81	145	−710	74.8
35	0	9.42	99	−686		0	4.40	98	−712	
	50	6.02	118	−685	36.1	50	2.92	119	−712	33.6
	250	4.68	125	−685	50.3	100	2.50	129	−709	43.2
	400	3.51	137	−684	62.7	200	1.44	135	−707	67.3
	600	2.42	149	−682	74.3	250	1.20	142	−706	72.7
40	0	9.82	80	−693		0	5.91	74	−723	
	50	6.33	102	−692	35.5	50	4.33	113	−723	26.7
	250	5.10	115	−690	48.1	100	3.54	121	−720	40.1
	400	3.94	133	−687	59.9	200	2.59	135	−719	56.2
	600	2.73	141	−686	72.2	250	2.20	133	−719	62.8
45	0	12.51	71	−699		0	6.84	70	−725	
	50	8.94	96	−698	28.5	50	5.68	110	−725	16.9
	250	8.03	118	−693	35.8	100	4.86	120	−723	28.9
	400	6.42	126	−691	48.7	200	3.81	124	−722	44.3
	600	5.18	132	−690	58.6	250	3.58	133	−721	47.7
50	0	15.60	64	−703		0	7.88	65	−727	
	50	11.53	91	−703	26.1	50	6.75	105	−727	14.3
	250	10.00	101	−701	35.9	100	6.41	116	−726	18.7
	400	8.32	113	−698	46.7	200	5.20	119	−724	34.0
	600	7.51	118	−697	51.8	250	4.55	122	−720	42.3

Table 4
Electrochemical parameters obtained from PDP measurements of Al composite and its base alloy in 0.5 M hydrochloric acid and 0.25 M sulphuric acid mixture in absence and presence of various concentrations of DMABT.

Temp. of medium (°C)	Composite					Base alloy				
	Conc. of inhibitor (ppm)	I_{cor} ($\times_{10}{}^{-3}$ A cm^{-2})	$-b_c$ (mV dec^{-1})	E_{corr} (mV SCE^{-1})	IE%	Conc. of inhibitor (ppm)	I_{cor} ($\times_{10}{}^{-4}$ A cm^{-2})	$-b_c$ (mV dec^{-1})	E_{corr} (mV SCE^{-1})	IE%
30	0	2.32	87	−643		0	5.24	96	−667	
	50	1.76	100	−653	24.1	50	4.15	100	−669	20.8
	100	1.46	107	−659	37.1	100	3.46	105	−669	33.9
	200	1.15	113	−655	50.4	200	3.00	107	−671	42.7
	300	0.86	115	−662	62.9	250	2.78	108	−673	46.9
35	0	2.61	83	−649		0	6.85	83	−669	
	50	2.03	98	−656	22.2	50	5.48	96	−670	20.0
	100	1.71	104	−657	34.5	100	4.80	96	−670	29.9
	200	1.34	107	−660	48.7	200	4.12	102	−673	39.8
	300	1.00	106	−666	61.7	250	3.70	104	−675	46.0
40	0	3.83	80	−658		0	7.25	74	−678	
	50	3.01	91	−658	21.4	50	5.87	89	−678	19.0
	100	2.68	99	−660	30.0	100	5.32	92	−679	26.6
	200	2.11	101	−662	44.9	200	4.51	96	−682	37.8
	300	1.72	103	−666	55.1	250	4.05	99	−683	44.1
45	0	5.53	73	−664		0	10.03	66	−683	
	50	4.63	85	−668	16.3	50	8.51	80	−684	15.1
	100	4.12	96	−669	25.5	100	7.44	82	−684	25.8
	200	3.14	97	−675	43.6	200	6.60	87	−685	34.2
	300	2.53	100	−671	54.2	250	6.05	88	−687	39.7
50	0	7.81	63	−670		0	18.2	56	−690	
	50	6.63	81	−670	15.1	50	15.68	65	−690	13.8
	100	6.12	89	−673	21.6	100	14.33	67	−691	21.3
	200	4.49	94	−674	42.5	200	12.52	70	−693	30.6
	300	3.71	98	−676	52.5	250	11.63	74	−695	35.4

The surface coverage θ of the inhibitor at different inhibitor concentrations was calculated from the equation:

$$\theta = \frac{i_{corr}(\text{uninh}) - i_{corr}(\text{inh})}{i_{corr}(\text{uninh})} \quad (2)$$

Inhibition efficiency was then calculated using the equation:

$$\text{IE}\ \ (\%) = \theta \times 100 \quad (3)$$

The data in the tables clearly show that the addition of DMABT decreases the corrosion rates of both the composite and the base alloy. Inhibition efficiency increases with increasing DMABT concentration. It is also seen that the addition of DMABT does not significantly shift the E_{corr} values. Further it is seen from the data in Tables 2–4 and Figs. 1 and 2 that cathodic and anodic Tafel slopes change only slightly on the addition of DMABT. The above-described observations suggest that the inhibitor molecules are adsorbed on the surface of the composite/base alloy and mechanically block the metal surface from the action of corrosion media. The inhibitor decreases the surface area for corrosion without altering the mechanism of corrosion and only causes inactivation of part of the surface. This fact is an important observation, since the presence of SiC particles in the composite initiates cathodic sites is responsible for the higher corrosion of the composite than that of the base alloy [8,10]. Therefore blocking these sites via DMABT adsorption would result in decreasing the corrosion rate of composite to a greater extent as compared to the base alloy. The comparison of inhibition efficiency of DMABT for the composite and base alloy at different concentrations and different temperatures shows that the inhibition effect is more on the composite than on the base alloy. The increase in the efficiency of the inhibitor in the case of composite may be due to its heterogenic nature, where the incorporation of silicon carbide acts as the potential active site for the adsorption of the inhibitor. The increase in inhibition efficiency with increasing inhibitor concentration indicates that more inhibitor molecules are adsorbed on the metal surface, thus providing wider surface coverage.

Though the E_{corr} values do not show any appreciable shift, the data in the tables reveal that, at higher concentrations of acid mixtures (2 M + 1 M and 1 M + 0.5 M), the values are slightly shifted to positive direction and at lower concentration of acid mixture (0.5 M + 0.25 M), the shift is slightly shifted to the negative direction. Therefore DMABT acts as a mixed inhibitor with predominantly anodic action at higher concentration of acid mixture and with predominantly cathodic action at lower concentration of acid mixture [23,24]. This can probably be due to the higher adsorption of protonated DMABT molecules on the anodic sites at higher concentration of the acids. The results presented in the tables also reveal that inhibition efficiency of DMABT decreases with increase in temperature. The maximum attainable inhibition efficiency increases with increase in acid mixture concentration.

3.2. Electrochemical impedance spectroscopy (EIS) measurements

In order to gain more information about the corrosion inhibition phenomenon, electrochemical impedance spectroscopy measurements were carried out for the 6061 Al–SiC composite and its base alloy in three different concentrations of acid mixtures in the presence and absence of DMABT at different temperatures. Figs. 3 and 4 represent Nyquist plots of composite and its base alloy in the presence of various concentrations of DMABT in a solution containing 2 M hydrochloric acid and 1 M sulphuric acid mixture at 30 °C, respectively. Similar results were obtained in other two concentrations of acid mixture and also at other temperatures studied.

As can be seen from Figs. 3 and 4, the impedance diagrams show semicircles, indicating that the corrosion process is mainly charge transfer controlled. The general shape of the curve is similar for

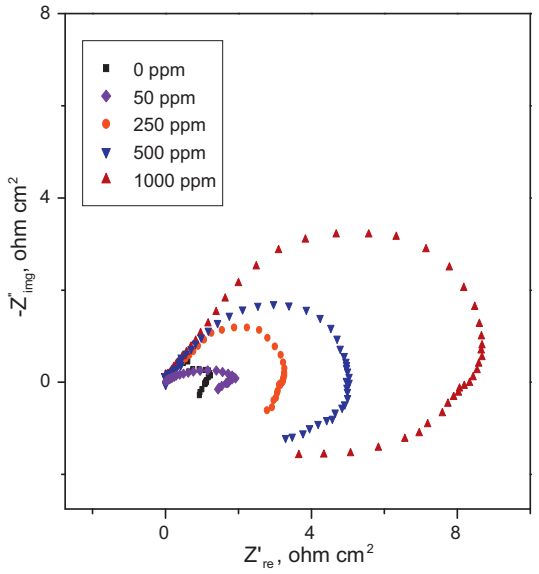

Fig. 3. Nyquist plots for the corrosion of composite in 2 M HCl + 1 M H_2SO_4 mixture at 30 °C in the presence of different concentrations of DMABT.

samples of the base alloy and composite, with large capacitive loop at high frequencies (HFs) and an inductive loop at low frequencies (LFs). Similar impedance plots have been reported in the literature for the corrosion of pure aluminum and aluminum alloys in various electrolytes such as sodium sulphate [25–27], sulphuric acid [26,27], acetic acid [26], sodium chloride [28,29] and hydrochloric acid [30–36].

The high frequency capacitive loop could be assigned to the charge transfer of the corrosion process and to the formation of oxide layer [37,38]. The oxide film is considered to be a parallel circuit of a resistor due to the ionic conduction in the oxide film and a capacitor due to its dielectric properties. According to Brett [31,33], the capacitive loop is corresponding to the interfacial reactions, particularly, the reaction of aluminum oxidation at the metal/oxide/electrolyte interface. The process includes the formation of Al^+ ions at the metal/oxide interface, and their migration through the oxide/solution interface where they are oxidized to Al^{3+}. At the oxide/solution interface, OH^- or O^{2-} ions are also formed. The fact that all the three processes are represented by only one loop could be attributed either to the overlapping of the loops of processes, or to the assumption that one process dominates and, therefore, excludes the other processes [27]. The other explanation offered to the high frequency capacitive loop is the oxide film itself. This was supported by a linear relationship between the inverse of the capacitance and the potential found by Bessone et al. [28] and Wit and Lenderink [27]. The origin of the inductive loop has often been attributed to surface or bulk relaxation of species in the oxide layer [29]. The LF inductive loop may be related to the relaxation process obtained by adsorption and incorporation of sulphate ions, oxide ion and charged intermediates on and into the oxide film [26].

The impedance parameters derived from Nyquist plots and inhibition efficiency of DMABT in 2 M hydrochloric acid and 1 M sulphuric acid mixture at different temperatures are given in Table 5. Similar results were obtained for other concentration of acid mixtures also. The measured values of polarization resistance increase with the increasing concentration of DMABT in the solution, indicating decrease in the corrosion rate for the composite and base alloy with increase in DMABT concentration. This is in accordance with the observations obtained from potentiodynamic measurements. However, the semicircles of the impedance spectra for the composite in the presence and in the absence of the inhibitor

Table 5
Electrochemical parameters obtained from EIS measurements of Al composite and its base alloy in 2 M hydrochloric acid and 1 M sulphuric acid mixture in the absence and presence of various concentrations of DMABT.

Temp. of medium (°C)	Composite						Base alloy					
	Conc. of inhibitor (ppm)	R_s (Ω cm^2)	R_p (Ω cm^2)	CPE ($\times 10^2$ μF)	n	IE%	Conc. of inhibitor (ppm)	R_s (Ω cm^2)	R_p (Ω cm^2)	CPE ($\times 10^1$ μF)	n	IE%
30	0	1.15	1.31	16.1	0.81		0	1.13	2.86	20.5	0.93	
	50	1.14	2.31	11.1	0.80	43.3	50	1.11	4.75	12.6	0.91	39.4
	250	1.18	3.00	9.9	0.82	56.3	100	1.13	6.25	11.2	0.94	54.2
	500	1.17	4.91	6.8	0.85	73.3	250	1.19	7.50	10.9	0.95	61.9
	1000	1.26	9.02	5.4	0.86	85.5	500	1.15	12.20	7.81	0.96	76.6
35	0	0.94	0.78	19.2	0.80		0	0.93	2.00	22.5	0.91	
	50	0.90	1.32	12.4	0.81	40.2	50	0.98	3.22	13.8	0.92	37.3
	250	0.98	1.60	10.1	0.83	51.3	100	0.91	3.95	12.4	0.94	49.4
	500	1.00	2.53	8.3	0.88	69.2	250	0.94	4.93	11.8	0.93	59.4
	1000	0.88	4.41	6.1	0.89	82.3	500	0.92	7.81	8.8	0.95	74.4
40	0	0.86	0.48	24.6	0.78		0	0.84	1.73	33.2	0.88	
	50	1.01	0.78	19.4	0.80	38.5	50	0.87	2.73	18.4	0.89	36.4
	250	0.93	0.92	17.9	0.85	47.5	100	0.88	3.01	16.6	0.90	42.5
	500	0.94	1.20	15.1	0.88	60.0	250	0.82	3.88	14.9	0.92	55.4
	1000	0.90	2.05	11.4	0.89	76.4	500	0.81	4.98	10.9	0.94	65.3
45	0	0.88	0.31	30.2	0.75		0	0.77	1.62	41.6	0.85	
	50	0.87	0.47	26.8	0.74	34.0	50	0.75	2.31	26.7	0.84	29.9
	250	0.92	0.58	24.2	0.79	43.0	100	0.71	2.66	23.3	0.87	39.1
	500	0.99	0.69	21.9	0.83	55.1	250	0.79	3.28	21.8	0.88	49.5
	1000	0.89	0.98	18.6	0.84	68.4	500	0.74	4.11	16.1	0.89	60.4
50	0	0.63	0.22	36.6	0.72		0	0.62	1.48	50.4	0.83	
	50	0.70	0.29	36.0	0.70	24.1	50	0.65	2.01	33.8	0.82	26.4
	250	0.68	0.33	35.4	0.71	33.3	100	0.69	2.38	32.4	0.85	33.2
	500	0.65	0.40	33.8	0.76	45.0	250	0.63	2.50	28.8	0.87	40.8
	1000	0.69	0.53	30.9	0.79	58.5	500	0.69	3.08	21.7	0.88	50.9

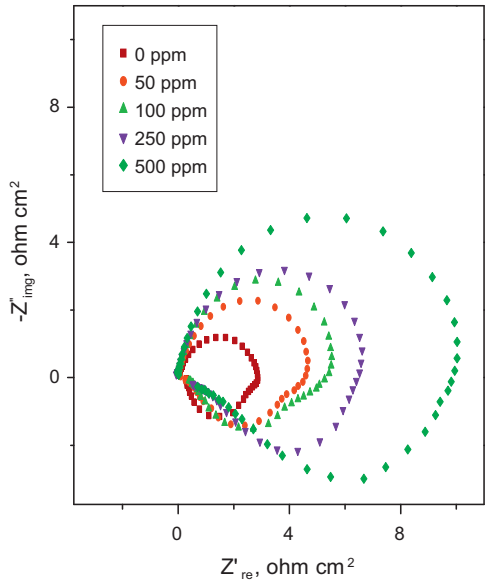

Fig. 4. Nyquist plots for the corrosion of base alloy in 2 M HCl + 1 M H_2SO_4 mixture at 30 °C in the presence of different concentrations of DMABT.

are depressed. Deviation of this kind is referred to as frequency dispersion, and has been attributed to inhomogeneties of solid surfaces, as the aluminum composite is reinforced with SiC particles. Mansfeld et al. [37,38] have suggested an exponent n in the impedance function as a deviation parameter from the ideal behavior. By this suggestion, the capacitor in the equivalent circuit can be replaced by a so-called constant phase element (CPE), which is a frequency-dependent element and related to surface roughness. The impedance function of a CPE has the following equation [26]:

$$Z_{CPE} = \frac{1}{(Y_0 j\omega)^n} \tag{4}$$

where the amplitude Y_0 and n are frequency independent, and ω is the angular frequency for which $-Z''$ reaches its maximum value, n is dependent on the surface morphology: $-1 \le n \le 1$. Y_0 and n can be calculated by the equations proved by Mansfeld et al. [39]. In the case of base alloy, due to the homogenous surface, frequency dispersion is very less. Therefore the obtained semicircles in the impedance spectra are not depressed.

An equivalent circuit of five elements depicted in Fig. 5 was used to simulate the measured impedance data on the composite and the base alloy. In this equivalent circuit, R_s is the solution resistance and R_t is the charge transfer resistance. R_L and L represent the inductive elements. This also consists of constant phase element, CPE (Q) in parallel to the parallel resistors R_t and R_L, and the latter is in series with the inductor L. When an inductive loop is present, the polarization resistance R_p can be calculated from [5]:

$$R_p = \frac{R_L \times R_t}{R_L + R_t} \tag{5}$$

Since R_p is inversely proportional to the corrosion current and it can be used to calculate the inhibition efficiency from the relation,

$$IE\% = \left(\frac{R'_p - R_p}{R'}\right) \times 100 \tag{6}$$

where R'_p and R_p are the polarization resistances in the presence and absence of inhibitors.

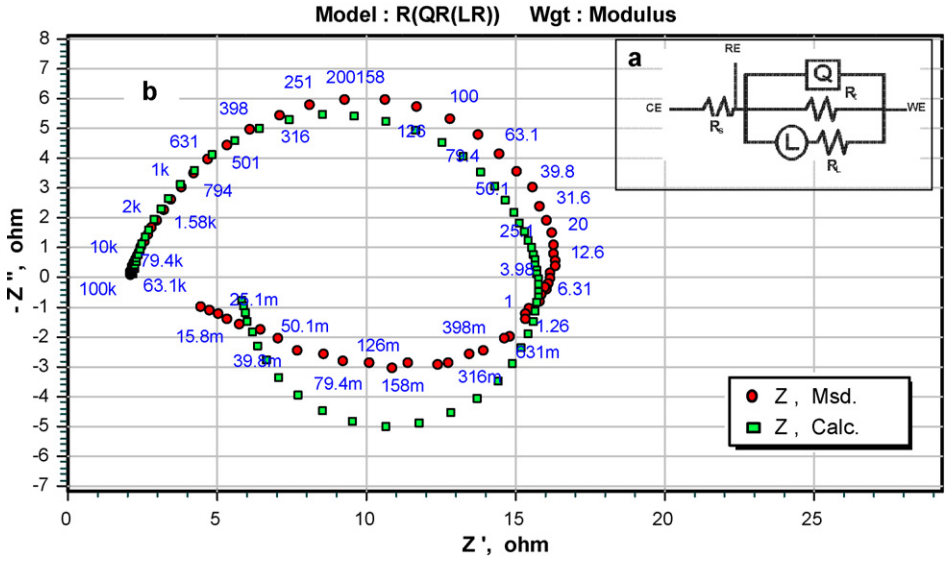

Fig. 5. The equivalent circuit model used to fit the experimental data.

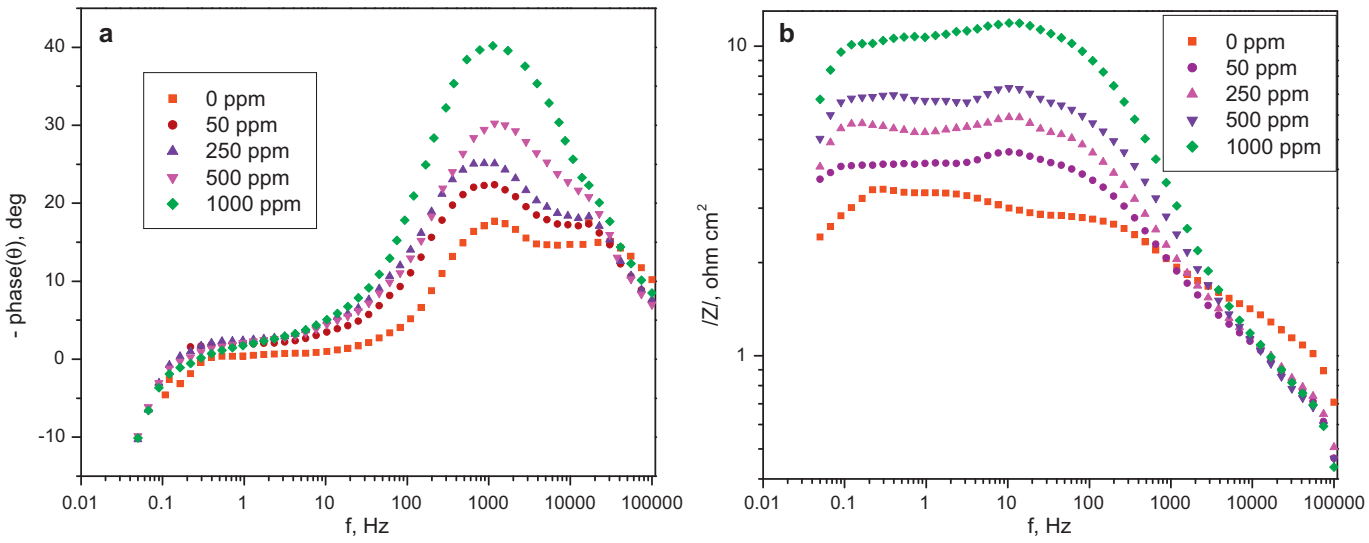

Fig. 6. (a) Bode phase plots for the corrosion of composite in 2 M HCl + 1 M H_2SO_4 mixture at 30 °C in the presence of different concentrations of DMABT. (b) Bode magnitude plots for the corrosion of composite in 2 M HCl + 1 M H_2SO_4 mixture at 30 °C in the presence of different concentrations of DMABT.

The Bode plots (Bode phase plots and Bode magnitude plots) obtained at OCP for 6061 Al/SiC composite and its base alloy with and without inhibitor containing 2 M hydrochloric acid and 1 M sulphuric acid mixture obtained at 30 °C are presented in Figs. 6 and 7, respectively. It is apparent that, for both the composite and the base alloy, the values of phase increase with increase in concentration of added DMABT up to their optimal concentration.

The Bode magnitude plots indicate the presence of only one slope for the uninhibited and inhibited systems. The difference between the high frequency (HF) limit and low frequency (LF) limit in the bode plot is equal to R_p, the polarization resistance, which is associated with the dissolution and repassivation processes occurring at the interface as well as the electronic conductivity of the film. The difference between the HF and LF for the uninhibited and inhibited systems in the Bode plot increases with increase in the concentration of DMABT up to their critical concentration.

It is seen from Table 5 that R_s (solution resistance) remains almost constant, with and without the addition of DMABT for both the composite and its base alloy. It was also observed that the value of constant phase element, Q, decreases, while the values of R_p and R_t increase with increasing concentration of DMABT, indicating that the inhibition efficiency increases with the increase in concentration of DMABT. A comparison of the inhibiting efficiencies obtained using ac and dc methods shows that an acceptable agreement in results is achieved in the two methods.

The double layer between the charged metal surface and the solution is considered as an electrical capacitor. The adsorption of DMABT on the aluminum surface decreases its electrical capacity because they displace the water molecules and other ions originally adsorbed on the surface. The decrease in this capacity with increase in DMABT concentrations may be attributed to the formation of a protective layer on the electrode surface. The thickness of this protective layer increases with increase in inhibitor concentration up to their critical concentration and then decreases. The obtained CPE (Q) values decrease noticeably with increase in the concentration of DMABT.

3.3. Adsorption isotherm considerations

In order to understand the mechanism of corrosion inhibition, the adsorption behavior of the organic adsorbate on the

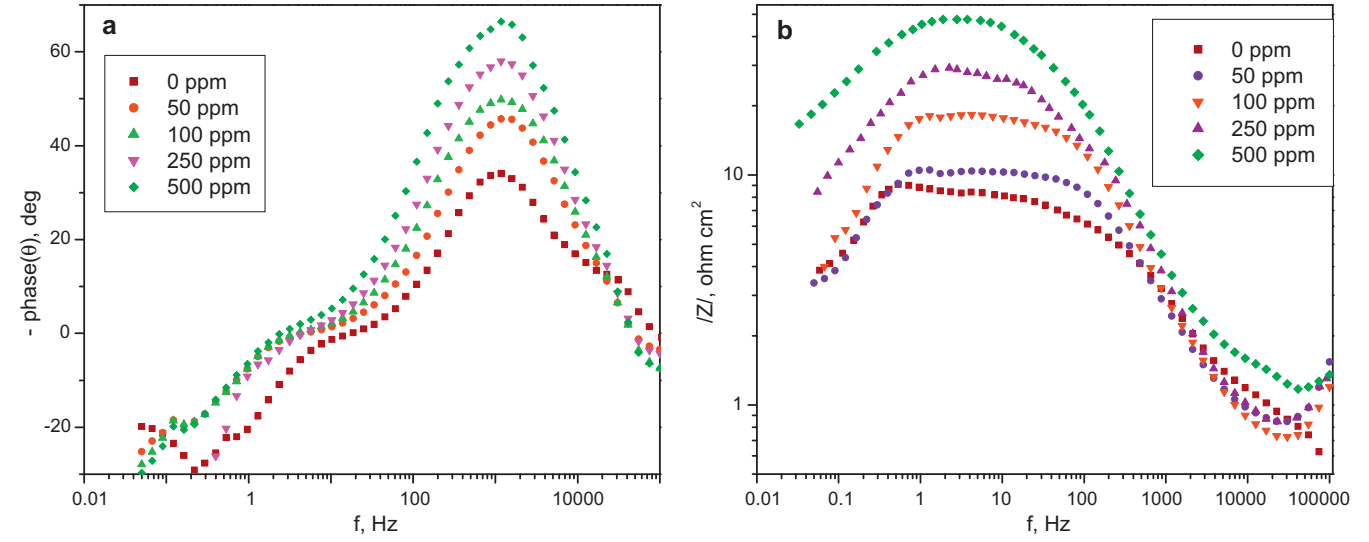

Fig. 7. (a) Bode phase plots for the corrosion of base alloy in 2 M HCl + 1 M H_2SO_4 mixture at 30 °C in the presence of different concentrations of DMABT. (b) Bode magnitude plots for the corrosion of base alloy in 2 M HCl + 1 M H_2SO_4 mixture at 30 °C in the presence of different concentrations of DMABT.

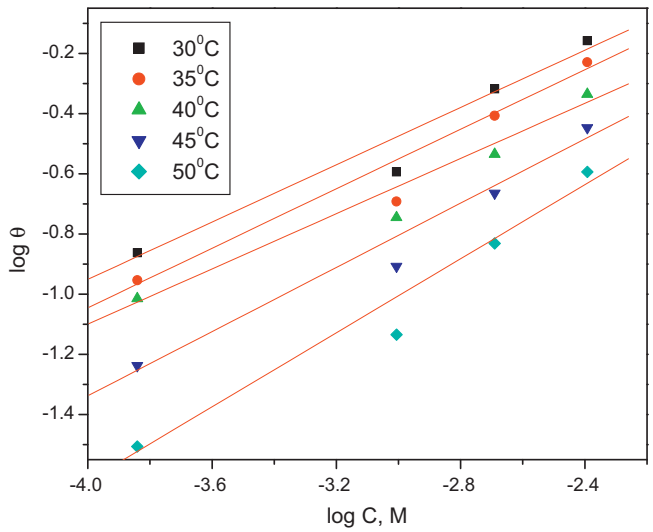

Fig. 8. Curve fitting of corrosion data for the composite in 2 M HCl + 1 M H_2SO_4 mixture in the presence of different concentrations of the DMABT to Frumkin adsorption isotherm.

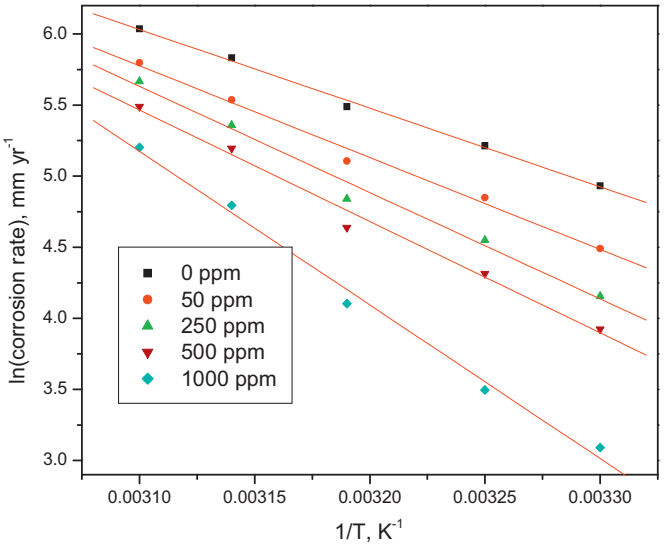

Fig. 10. Arrhenius plots for the composite in 2 M HCl + 1 M H_2SO_4 mixture at different concentrations of DMABT.

aluminum surface must be known. The degree of surface coverage (θ) for different concentrations of inhibitor was evaluated from potentiodynamic polarization measurements. The data were tested graphically by fitting to various isotherms. Freundlich adsorption isotherm was found to be the best description for the adsorption behavior of the studied inhibitors. According to this isotherm, θ is related to the equilibrium adsorption constant (K) and concentration (C) of inhibitor in mol dm^{-3} as per the relation:

$$\theta = KC^n \tag{7}$$

where $0 < n < 1$. In logarithmic form Eq. (7) can be written as:

$$\log\theta = \log K + n\log C \tag{8}$$

Eq. (8) predicts that a plot of $\log\theta$ versus $\log C$ will be linear.

Figs. 8 and 9 show the Freundlich adsorption isotherms for the composite and the base alloy, respectively. From the slope the value of n was calculated and the value of n is $0 < n < 1$ which confirms the applicability of Freundlich isotherm.

The free energy of adsorption, ΔG_{ads}, was calculated using the relation,

$$\Delta G_{ads} = -RT\ln\left[\frac{55.5\theta}{C(1-\theta)}\right] \tag{9}$$

where C is the concentration of the inhibitor expressed in mol dm^{-3}. The calculated values of ΔG_{ads} for DMABT on the composite and the base alloy were in the range of −26.37 to −31.0 kJ mol^{-1} and −27.1 to 30.4 kJ mol^{-1}, respectively. The negative values of ΔG_{ads} suggest the spontaneous adsorption of DMABT on the composite and base alloy surfaces. Since the values of ΔG_{ads} of −40 kJ mol^{-1} are usually accepted as threshold value between chemisorption and physisorption, the obtained values of the ΔG_{ads} may be indicative of physical adsorption [34].

The corrosion inhibition property of DMABT through adsorption on the surface of the composite or the base alloy can be attributed to the presence of electronegative elements such as nitrogen and sulphur and also to the presence of π electrons on

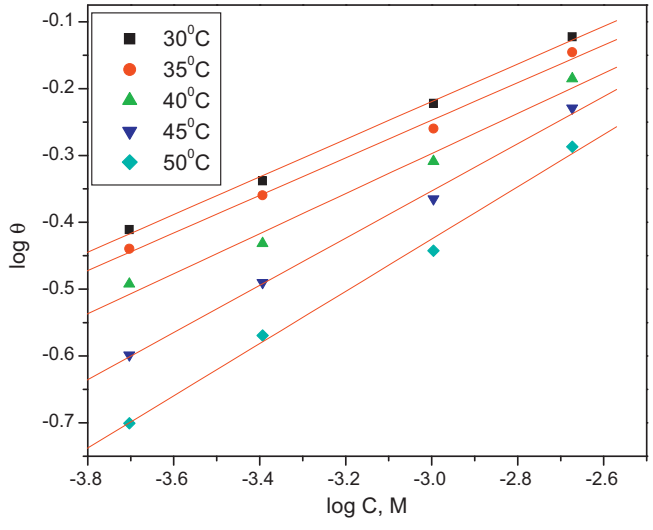

Fig. 9. Curve fitting of corrosion data for the base alloy in 2 M HCl + 1 M H_2SO_4 mixture in the presence of different concentrations of the DMABT to Frumkin adsorption isotherm.

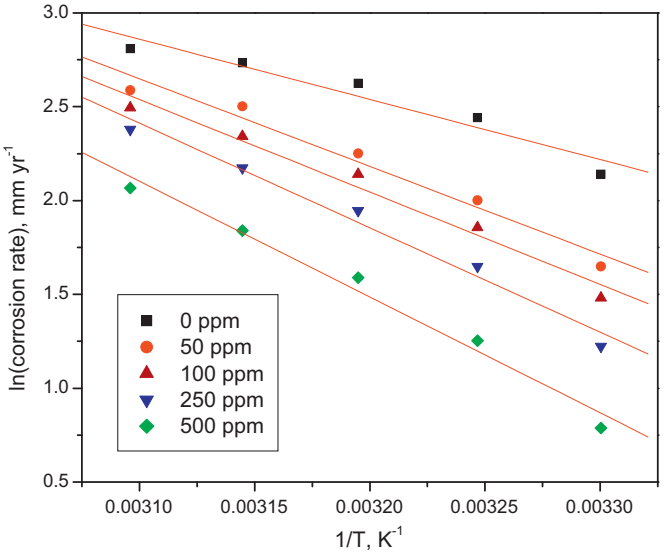

Fig. 11. Arrhenius plots for the base alloy in 2 M HCl + 1 M H_2SO_4 acid mixture at different concentrations of DMABT.

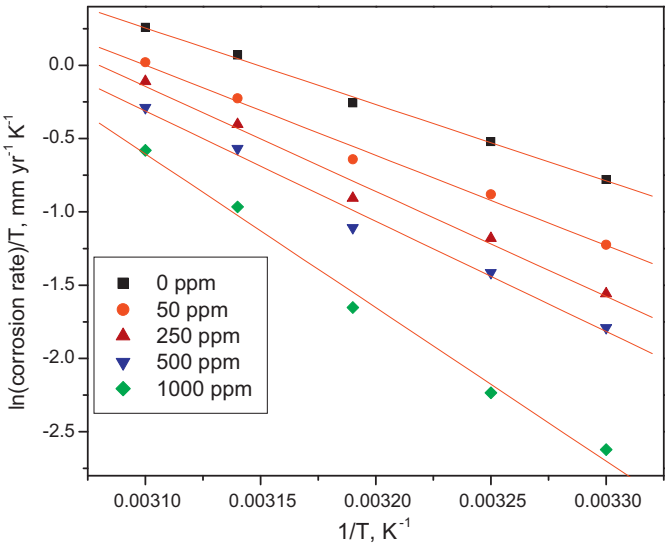

Fig. 12. ln(corrosion rate/T) versus $1/T$ for composite in 2 M HCl + 1 M H_2SO_4 at different concentrations of DMABT.

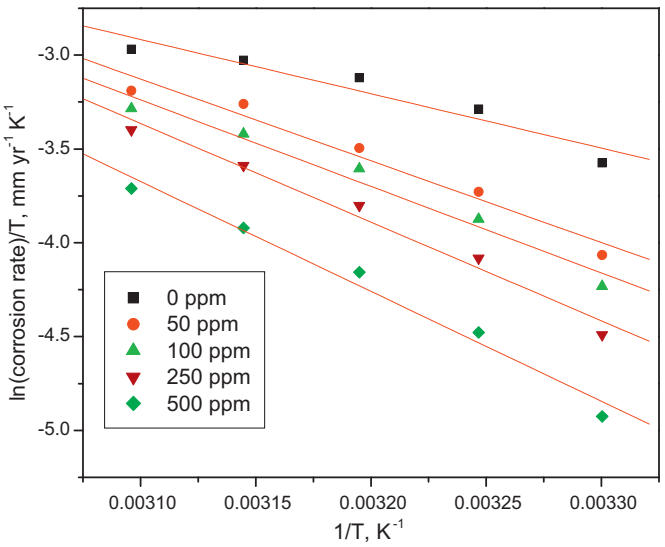

Fig. 13. ln(corrosion rate/T) versus $1/T$ for base alloy in 2 M HCl + 1 M H_2SO_4 at different concentrations of DMABT.

the benzene ring. The metal surface in contact with a solution is charged due to the electric field that emerges at the interface on the immersion in the electrolyte. This can be determined, according to Antropov et al. [40], by comparing the zero charge potential and the rest potential of the metal in the corresponding medium. The value of pH_{Zch}, which is defined as the pH at a point of zero charge is equal to 9.1 for aluminum [41]. So aluminum is positively charged in highly acidic medium, as the ones used in this investigation. Therefore, chloride ions, sulphate ions and DMABT can be adsorbed on aluminum surface via their negative centres. Also, DMABT can be protonated in the highly acidic solution used in the investigation. The mechanism of adsorption of protonated DMABT can be predicted on the basis of the mechanism proposed for the corrosion of aluminum in hydrochloric acid [42]. According to this mechanism, anodic dissolution of Al follows steps

$$Al + Cl \rightleftharpoons AlCl^- \quad (10)$$

$$AlCl^-{}_{(ads)} + Cl^- \rightarrow AlCl_2{}^+ + 3e^- \quad (11)$$

The cathodic hydrogen evolution is according to the following steps

$$H^+ + e^- \rightarrow H_{(ads)} \quad (12)$$

$$H_{(ads)} + H_{(ads)} \rightarrow H_2 \quad (13)$$

Protonated DMABT can electrostatically interact with $AlCl^-{}_{(ads)}$ species, and then the oxidation of $AlCl^-{}_{(ads)}$ to $AlCl_2{}^+$ as shown in Eq. (11) can be prevented. This phenomenon is expected for the stabilization of adsorbed halide ions by means of electrostatic interactions with the inhibitor molecules resulting in greater surface charges [43,44]. The protonated molecules can also adsorb on the cathodic sites of aluminum in competition with the hydrogen ions (Eq. (10)). DMABT can also be adsorbed from its negatively charged centres such as nitrogen and sulphur atom to positively charged cathodic sites.

3.4. Effect of temperature and activation parameters of inhibition process

The results of potentiodynamic polarization and electrochemical impedance spectroscopy given in Tables 2–5 indicate that

Table 6
Activation parameters of the corrosion of 6061 Al–SiC composite in the absence and presence of different concentrations of DMABT.

Activation parameters	Concentration of the medium in M														
	2 M HCl + 1 M H_2SO_4 Inhibitor concentration (ppm)					1 M HCl + 0.5 M H_2SO_4 Inhibitor concentration (ppm)					0.5 M HCl + 0.25 M H_2SO_4 Inhibitor concentration (ppm)				
	0	50	250	500	1000	0	50	250	400	600	0	50	100	200	300
E_a (kJ mol^{-1})	47.3	53.7	62.2	65.1	89.8	60.4	64.0	65.4	66.3	90.6	66.2	70.1	72.7	75.0	91.2
ΔH (kJ mol^{-1})	44.7	51.1	59.6	62.5	87.1	53.2	62.1	62.7	63.6	87.8	64.1	67.8	70.5	73.0	89.0
ΔS (J mol^{-1} K^{-1})	54.9	72.3	97.3	105.6	179.6	55.7	77.3	98.1	117.2	181.4	82.3	88.1	90.6	120.3	182.6

Table 7
Activation parameters of the corrosion of 6061 base alloy in the absence and presence of different concentrations of DMABT.

Activation parameters	Concentration of the medium in M														
	2 M HCl + 1 M H_2SO_4 Inhibitor concentration (ppm)					1 M HCl + 0.5 M H_2SO_4 Inhibitor concentration (ppm)					0.5 M HCl + 0.25 M H_2SO_4 Inhibitor concentration (ppm)				
	0	50	100	250	500	0	50	100	200	250	0	50	100	200	250
E_a (kJ mol^{-1})	23.8	39.6	40.7	42.9	47.9	32.3	39.9	42.3	47.9	53.0	48.4	52.3	55.2	56.2	57.4
ΔH (kJ mol^{-1})	21.2	38.1	36.9	40.3	45.3	31.2	38.5	40.8	45.7	51.2	46.7	49.7	53.0	53.9	54.2
ΔS (J mol^{-1} K^{-1})	−44.0	2.2	7.1	11.2	24.1	−7.1	39.9	54.9	57.4	60.7	40.7	51.5	59.9	61.5	65.6

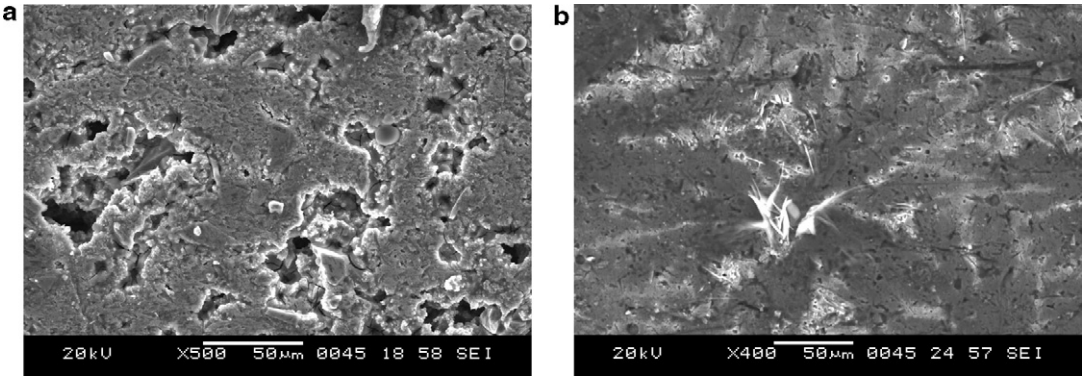

Fig. 14. (a) SEM image of the surface of composite after immersion for 2 h in 2 M HCl + 1 M H_2SO_4 at 30 °C. (b) SEM image of the surface of composite after immersion for 2 h in 2 M HCl + 1 M H_2SO_4 at 30 °C in the presence of 1000 ppm of DMABT.

inhibition efficiency of DMABT on both the composite and the base alloy decreases with increase in temperature. This may be attributed to the higher dissolution rates of aluminum at elevated temperature and also a possible desorption of adsorbed inhibitor due to increased solution agitation resulting from higher rates of hydrogen gas evolution, which may also reduce the ability of the inhibitor to be adsorbed on the metal surface. Such behavior which was observed in both samples, suggests physical adsorption of the DMABT on the corroding aluminum surface [45,46].

Plot of log (corrosion rate) versus $1/T$ for both samples of composite and base alloy in the acid mixture containing 2 M hydrochloric acid and 1 M sulphuric acid in the absence and presence of various concentrations of DMABT is shown in Figs. 10 and 11. As shown in these figures, straight lines were obtained according to Arrhenius-type equation:

$$\log(\text{corrosion rate}) = \log A - \frac{E_a}{2.303RT} \tag{14}$$

where A is a constant and depends on metal type and electrolyte, E_a is the apparent activation energy, R is the universal gas constant and T is the absolute temperature.

Plot of log (corrosion rate/T) versus $1/T$ for both the samples of composite and base alloy in the acid mixture containing 2 M hydrochloric acid and 1 M sulphuric acid in the absence and presence of various concentrations of DMABT is shown in Figs. 12 and 13. As shown in these figures, straight lines were obtained according to transition state equation:

$$\text{Corrosion rate} = \frac{RT}{Nh} \cdot e^{\Delta S/R} \cdot e^{-\Delta H/RT} \tag{15}$$

where h is Planck's constant, N is Avogadro′s number, ΔH is the change in the enthalpy of activation and ΔS is the change in entropy of activation. The calculated values of E_a, ΔH, ΔS are given in Tables 6 and 7. The data in the tables show that the values of E_a of the corrosion of composite and base alloy in the acid mixture medium in the presence of DMABT are higher than those in the uninhibited medium. The increase in the E_a values, with increasing inhibitor concentration indicates the increase in energy barrier for the corrosion reaction, with the increasing concentrations of the inhibitor. The values of E_a are higher for the composite than for the base alloy. The increase in the activation energies with increasing concentration of the inhibitor is attributed to physical adsorption of inhibitor molecules on the metal surface [47], with an appreciable increase in the adsorption process of the inhibitor on the metal surface with increase in the concentration of inhibitor. The adsorption of the inhibitor molecules on the surface of the alloy blocks the charge transfer during corrosion reaction, thereby increasing the activation energy [48]. In other words, the adsorption of the inhibitor on the electrode surface leads to the formation of a physical barrier that reduces the metal reactivity in the electrochemical reactions of corrosion [49]. In the case of both the samples of aluminum, the inhibition efficiency decreases with increase in temperature which indicates desorption of inhibitor molecule as the temperature increases [50].

The values of ΔS are higher for inhibited solutions than those for the uninhibited solutions. This suggested that an increase in randomness occurred on going from reactants to the activated complex. This might be the results of the adsorption of organic inhibitor molecules from the acidic solution which could be regarded as a quasi-substitution process between the organic compound in the aqueous phase and water molecules at electrode surface [51]. In

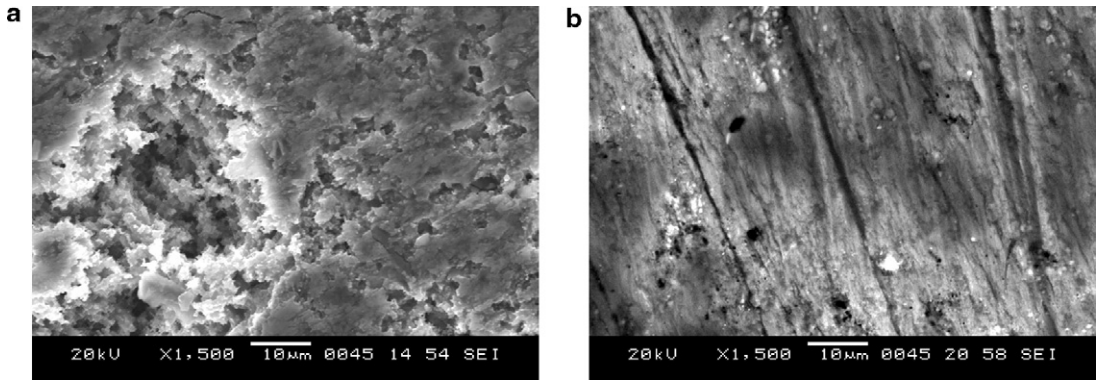

Fig. 15. (a) SEM image of the surface of base alloy after immersion for 2 h in 2 M HCl + 1 M H_2SO_4 at 30 °C. (b) SEM image of the surface of composite after immersion for 2 h in 2 M HCl + 1 M H_2SO_4 at 30 °C in the presence of 500 ppm of DMABT.

this situation, the adsorption of organic inhibitor is accompanied by desorption of water molecules from the surface. Thus the increase in entropy of activation was attributed to the increase in solvent entropy [52].

3.5. Scanning electron microscopy

In order to evaluate the effect of corrosion on the surface morphology of the composite and the base alloy, SEM analysis was carried out on the samples subjected to corrosion in acid mixture containing 2 M hydrochloric acid and 1 M sulphuric acid in the presence and absence of the inhibitors. Figs. 14 and 15 show the SEM images of the composite and base alloy, respectively. Fig. 14a shows deep cavities formed due to detachment of SiC particle from the composite when exposed to the acid mixture medium. This may be attributed to the corrosion at the interface between the particle and matrix due to the galvanic action, with the particle acting as a cathodic site and resulting in the detachment of the particle from the matrix. The faceting seen in Fig. 15a is a result of more or less uniform corrosion on the surface of the base alloy when exposed to the acid mixture medium. Figs. 14b and 15b show more or less smooth surfaces of the composite and the base alloy, without pits in the presence of inhibitors. It can be concluded that the adsorbed layer of inhibitor provides a corrosion free smooth surface with the lines of mechanical polishing on the composite and base alloy.

In order to gain information about the surface composition of the composite and base alloy, EDX studies were carried out on samples that were exposed to the corrosion medium in the presence and absence of the inhibitor. EDX spectra of the composite sample exposed to the acid mixture corrosion medium in the absence of inhibitor showed spectral lines corresponding to aluminum, silicon, oxygen and small peaks corresponding to sulphur and chlorine. In the spectra of the base alloy, the sulphur and chlorine peaks were negligibly small. The samples exposed to corrosion medium in the presence of inhibitors showed additional carbon and nitrogen signals, indicating surface coverage by the inhibitor. Presence of higher percentage of carbon and nitrogen on the surface of the composite samples than on base alloy reveals the higher adsorption of DMABT on the composite than on the base alloy. This also accounts for higher inhibition efficiency achieved on composite sample than on the base alloy sample.

4. Conclusions

1. DMABT acts as a good corrosion inhibitor for 6061 Al–15 vol. pct. $SiC_{(p)}$ composite and its base alloy in an acid medium containing sulphuric acid and hydrochloric acid.
2. Corrosion inhibition efficiency of DMABT increases with increasing concentration up to critical concentration.
3. DMABT acts as a mixed type inhibitor.
4. Inhibition efficiency of DMABT on aluminum composite and its base alloy increases with increase in concentration of acid mixture and decreases with increase in temperature from 30 °C to 50 °C.
5. Inhibitor obeys Freundlich model of adsorption and the adsorption is through physisorption.
6. Inhibition efficiency is higher on the composite than on the base alloy.

References

[1] I.M. Hutchings, S. Wilson, A.T. Alpas, in: T.W. Clyne (Ed.), Comprehensive Composite Materials, vol. 3, Elsevier Science Ltd., UK, 2000.
[2] D.M. Aylor, Corrosion of Metal Matrix Composites, Metals Hand Book, vol. 13, ninth ed., ASM, 1987.
[3] T.H. Sanders Jr., E.A. Starke Jr., Proceedings of the Fifth International Conference on Al–Lithium alloys, Materials & Composites Engineering Publications Ltd., Birmingham, UK, 1989, p. 1.
[4] C. Monticelli, F. Zucchi, G. Brunoro, G. Trabanelli, J. Appl. Electrochem. 27 (1997) 325.
[5] A. Pardo, M.C. Merino, S. Merino, F. Viejo, M. Carboneras, R. Arrabal, Corros. Sci. 47 (2005) 1750.
[6] C.E. Da Costa, F. Velasco, J.M. Toralba, Rev. Metal. Madrid 36 (2000) 179.
[7] P.K. Rohatgi, JOM 43 (1991) 10.
[8] A. Pardo, M.C. Merino, S. Merino, M.D. Lopez, F. Viejo, M. Carboneras, Mater. Corros. 54 (2003) 311.
[9] C.J. Peel, R. Moreton, P.J. Gregson, E.P. Hunt, Proceedings of the XIII International Conference on Society of Advanced Material and Process Engineering, SAMPE, Covina, CA, 1991, p. 189.
[10] A.J. Trowsdale, B. Noble, S.J. Haris, I.S.R. Gibbins, G.E. Thomson, G.C. Wood, Corros. Sci. 38 (1996) 177.
[11] F. Bentiss, Treisnel, M. Lagrence, Br. Corros. J. 35 (2000) 315.
[12] S.A. Rao, Padmalatha, J. Nayak, A.N. Shetty, J. Met. Mater. Sci. 47 (2005) 51.
[13] S.I. Pyun, K.H. Na, W.J. Lee, J.J. Park, Corrosion 56 (2000) 1015.
[14] M.N. Desai, S.S. Rana, M.H. Gandhi, Anticorros. Methods Mater. 18 (1971) 19.
[15] T.L. Rama Char, O.K. Padma, Trans. Inst. Chern. Engnrs. 47 (1969) 177.
[16] I.N. Putilova, S.A. Balezin, B. Arannik, Metallic Corrosion Inhibitors, Pergamon, Oxford, 1960, p. 67.
[17] G. Trabanelli, V. Carassiti, Advances in Corrosion Science and Technology, vol. 1, Plenum Press, New York, 1970, p. 147.
[18] I.L. Rozerfeld, Corrosion Inhibitors, McGraw Hill, New York, 1981, p. 147.
[19] C.C. Nathan, Corrosion Inhibitors, NACE, Houston, 1973, p. 7.
[20] F. Hunkeler, H. Bohni, Mater. Corros. 34 (1983) 68.
[21] Yu.J. Kuznetsov, Prot. Met. 20 (1984) 282.
[22] P.T. Shah, T.C. Daniels, Rev. Trav. Chim. 69 (1950) 1545.
[23] A. Yurt, S. Ulutas, H. Dal, Appl. Surf. Sci. 253 (2006) 919.
[24] A. El-Sayed, Corros. Prev. Control 43 (1996) 23.
[25] S. Sayed, Abdel Rehim, H. Hamdi Hassan, A. Mohammed Amin, Appl. Surf. Sci. 187 (2002) 187.
[26] H.J.W. Lenderink, M.V.D. Linden, J.H.W. De Wit, Electrochim. Acta 38 (1989) 1993.
[27] J.H. Wit, H.J.W. Lenderink, Electrochim. Acta 41 (1996) 1111.
[28] J.B. Bessone, D.R. Salinas, C. Mayer, M. Ebert, W.J. Lorenz, Electrochim. Acta 37 (1992) 2283.
[29] S.E. Frers, M.M. Stefenel, C. Mayer, T. Chierchie, J. Appl. Electrochem. 20 (1990) 996.
[30] M. Metikos-Hukovic, R. Babic, Z. Grubac, J. Appl. Electrochem. 28 (1998) 433.
[31] C.M.A. Brett, J. Appl. Electrochem. 20 (1990) 1000.
[32] E.J. Lee, S.I. Pyun, Corros. Sci. 37 (1995) 157.
[33] C.M.A. Brett, Corros. Sci. 33 (1992) 203.
[34] K.F. Khaled, M.M. Al-Qahtani, Mater. Chem. Phys. 113 (2009) 150.
[35] A. Ehteram Noor, Mater. Chem. Phys. 114 (2009) 533.
[36] A. Aytac, U. Ozmen, M. Kabasakaloglu, Mater. Chem. Phys. 89 (2005) 176.
[37] F. Mansfeld, S. Lin, K. Kim, H. Shih, Corros. Sci. 27 (1987) 997.
[38] F. Mansfeld, S. Lin, S. Kim, H. Shih, Mater. Corros. 39 (1988) 487.
[39] F. Mansfeld, C.H. Tsai, H. Shih, in: R.S. Munn (Ed.), Computer Modeling in Corrosion, ASTM, Philadelphia, PA, 1992, p. 86.
[40] L.I. Antropov, E.M. Makushin, V.F. Panasenko, Metallic Corrosion Inhibitors, Kiev, Technika, 1981, p. 182.
[41] M. Tschapek, C. Wasowski, R.M. Torres Sanchez, J. Electroanal. Chem. 74 (1976) 167.
[42] A.A. Awady, B.A. Abd. El-Nabey, S.G. Aziz, J. Chem. Soc., Faraday Trans. 84 (1993) 795.
[43] E.E. Oguzie, B.N. Okolue, C. Unaegbu, C.E. Ogukwe, A.I. Onuchukwu, Mater. Chem. Phys. 84 (2004) 363.
[44] G.K. Gomma, Mater. Chem. Phys. 55 (1998) 241.
[45] M. Abdallah, Corros. Sci. 46 (2004) 1981.
[46] E.E. Oguzie, Corros. Sci. 49 (2007) 1527.
[47] H. Ashassi-Sorkhabi, B. Shaabani, D. Seifzadeh, Appl. Surf. Sci. 239 (2005) 154.
[48] M.M. Osman, R.A. El-Ghazawy, A.M. Al-Sabagh, Mater. Chem. Phys. 80 (2003) 55.
[49] F. Mansfeld, Corrosion Mechanism, Marcel Dekkar, New York, 1987, p. 119.
[50] M.A. Ashish Kumar Singh, M.A. Quraishi, Corros. Sci. 52 (2010) 156.
[51] M. Sahin, S. Bilgic, H. Yilmaz, Appl. Surf. Sci. 195 (2002) 1.
[52] B. Ateya, B.E. El-Anadouli, F.M. El-Nizamy, Corros. Sci. 24 (1984) 509.